Functional Connectivity From Disease Epicenters in Frontotemporal Dementia

Federica Agosta, MD, PhD, Edoardo Gioele Spinelli, MD, Silvia Basaia, PhD, Camilla Cividini, MSc,
Francesco Falbo, MD, Costanza Pavone, MD, Nilo Riva, MD, PhD, Elisa Canu, PhD, Veronica Castelnovo, MSc,
Giuseppe Magnani, MD, Francesca Caso, MD, PhD, Paola Caroppo, MD, PhD, Sara Prioni, MSc,
Cristina Villa, PhD, Lucio Tremolizzo, MD, Ildebrando Appollonio, MD, Vincenzo Silani, MD,
Keith A. Josephs, MD, MST, MSc, Jennifer Whitwell, PhD, and Massimo Filippi, MD

Correspondence
Dr. Agosta
agosta.federica@hsr.it

Abstract

Background and Objectives

MRI connectomics is an ideal tool to test a network-based model of pathologic propagation from a disease epicenter in neurodegenerative disorders. In this study, we used a novel graph theory–based MRI paradigm to explore functional connectivity reorganization, discerning between direct and indirect connections from disease epicenters, and its relationship with neurodegeneration across clinical presentations of the frontotemporal dementia (FTD) spectrum, including behavioral variant of FTD (bvFTD), nonfluent variant of primary progressive aphasia (nfvPPA), and semantic variant of primary progressive aphasia (svPPA).

Methods

In this observational cross-sectional study, disease epicenters were defined as the peaks of atrophy of a cohort of patients with high confidence of frontotemporal lobar degeneration pathology (Mayo Clinic). These were used as seed regions for stepwise functional connectivity (SFC) analyses in an independent (Milan) set of patients with FTD to assess connectivity in regions directly and indirectly connected to the epicenters. Correlations between SFC architecture in healthy conditions and atrophy patterns in patients with FTD were also tested.

Results

As defined by comparing the 42 Mayo Clinic patients with 15 controls, disease epicenters were the left anterior insula for bvFTD, left supplementary motor area for nfvPPA, and left inferior temporal gyrus (ITG) for svPPA. Compared with 94 age-matched controls, patients with bvFTD (n = 64) and nfvPPA (n = 34) of the Milan cohort showed widespread decreased SFC in bilateral cortical regions with direct/indirect connections with epicenters and increased SFC either in directly connected regions, physically close to the respective seed region, or in more distant cortical/cerebellar areas with indirect connections. Across all link steps, svPPA (n = 36) showed SFC decrease mostly within the temporal lobes, with co-occurrent SFC increase in cerebellar regions at indirect link steps. The average stepwise topological distance from the left ITG in a reference group of 50 young healthy controls correlated with regional gray matter volume in svPPA, consistent with network-based degeneration.

Discussion

Our findings demonstrate that each FTD syndrome is associated with a characteristic interplay of decreased and increased functional connectivity with the disease epicenter, affecting both

Glossary

3D = 3-dimensional; **AAL** = Automated Anatomical Labeling; **AI** = anterior insula; **ANOVA** = analysis of variance; **bvFTD** = behavioral variant of FTD; **CDR** = Clinical Dementia Rating; **FTD** = frontotemporal dementia; **FTLD** = frontotemporal lobar degeneration; **FWE** = family-wise error; **GM** = gray matter; **ITG** = inferior temporal gyrus; **MMSE** = Mini-Mental State Examination; **nfvPPA** = nonfluent/agrammatic variant primary progressive aphasia; **ROI** = region of interest; **RS fMRI** = resting-state functional MRI; **SFC** = stepwise functional connectivity; **SMA** = supplementary motor area; **svPPA** = semantic variant primary progressive aphasia; **VBM** = voxel-based morphometry.

direct and indirect connections. SFC revealed novel insights regarding the topology of functional disconnection across FTD syndromes, holding the promise to be used to model disease progression in future longitudinal studies.

Frontotemporal dementia (FTD) includes a spectrum of heterogeneous neurodegenerative syndromes, including the behavioral variant of FTD (bvFTD),[1] nonfluent/agrammatic variant of primary progressive aphasia (nfvPPA), and semantic variant of primary progressive aphasia (svPPA).[2] Similar to other neurodegenerative diseases, FTD presentations are being increasingly conceptualized as "disconnection syndromes"[3,4] due to the disruption of brain network architectural organization causing the loss of an efficient balance between local (short range) and global (long range) connectivity, critical for an effective integration of information and adequate cognitive performance.[5] Such disruptive processes may start from disease-specific epicenters of neurodegeneration and subsequently spread through highly interconnected neural networks, as suggested by the overlap between atrophy patterns in patients with neurodegenerative conditions and large-scale connectivity networks in healthy controls.[6,7] MRI connectomics has demonstrated a close relationship between brain connectivity networks and atrophy accumulation in FTD,[8-11] supporting a "network-based" spread model of pathology. However, previous studies did not discern between direct and indirect connections with the disease epicenter. Stepwise functional connectivity (SFC) assesses functional connectivity modifications at different topological distances from a seed region of interest (ROI),[12,13] thus helping to discriminate between alterations of 1-step (direct) and longer-distance (indirect) connections. This validated framework[12] has recently demonstrated great potential for the study of neurodegenerative disorders in vivo.[13]

The main aim of this study was to evaluate SFC as a new approach to assess brain network disruption in FTD. In detail, we focused on exploring how the step distance functional connections of disease epicenters were altered in different clinical variants to provide novel insight into direct and downstream (i.e., indirect) effects of neurodegeneration over brain functional architecture. We have also investigated the relationship between SFC architecture of healthy controls and the atrophy distribution in each FTD group to test SFC as a determinant of pathologic progression.

Methods

Participants

Milan Cohort

A total of 176 patients with a suspected diagnosis of FTD disorders were referred between October 2009 and April 2021 to the Neurology Unit of San Raffaele Hospital in Milan to perform an optimized diagnostic protocol[14] including neurologic workup, neuropsychological evaluation, and 3T brain MRI. After this multidisciplinary evaluation, 157 patients received a clinical diagnosis of bvFTD, nfvPPA, or svPPA according to established criteria[1,2] and were evaluated for inclusion in this cross-sectional study. Exclusion criteria were as follows: substance abuse or any (other) major systemic, psychiatric, or neurologic illnesses; lacunae and extensive cerebrovascular disorders at MRI. To mitigate sources of sample heterogeneity, after screening for known pathogenic genetic variations (see Genetic Testing), 17 patients with known pathogenic genetic variations (i.e., 6 *C9orf72*, 9 *GRN*, 1 *MAPT*, and 1 *TREM2*) were excluded. Six patients with FTD (i.e., 1 bvFTD, 4 nfvPPA, and 1 svPPA), who demonstrated high cerebrovascular burden or motion artifacts on MRI, were also excluded. The final cohort included 134 patients with sporadic FTD, including 64 bvFTD, 34 nfvPPA, and 36 svPPA (Table 1). Ninety-six healthy controls, comparable for age and sex with patients (HC-old), were recruited among spouses of patients and by word of mouth. Controls had normal neurologic assessment, Mini-Mental State Examination (MMSE)[15] score ≥26, and no family history of neurodegenerative diseases. Fifty young healthy controls (HC-young, age range 20–30 years, 23 females) were also recruited, as a "reference" healthy connectome for correlation analyses between SFC maps and regional atrophy in patients with FTD, removing the influence of age-related connectome alterations.

Mayo Clinic Cohort

To identify the disease epicenters to be used as seeds of SFC analysis performed on the Milan cohort, MRI scans obtained from an independent group of individuals were also used. This population was recruited by the Neurodegenerative

Table 1 Demographic and Main Clinical Characteristics of Included Participants

Milan cohort

	HC-old	bvFTD	nfvPPA	svPPA	p Value
N	94	64	34	36	
Age at MRI, y	65.35 ± 6.39 (51.22–79.34)	65.92 ± 7.91 (45.51–79.76)	69.01 ± 8.3 (53.83–83.35)	66.94 ± 8.34 (48.46–81.63)	0.11
Sex, M/F	36/58	38/26	12/22	18/18	0.09
Education, y	12.51 ± 4.35 (5–24)[a]	9.65 ± 3.53 (3–17)	10.06 ± 5.8 (3–22)	11.83 ± 4.68 (3–18)	**0.001**
Disease duration, y	—	3.62 ± 2.25 (0.57–12.06)	2.55 ± 1.48 (0.13–6.17)[a,b]	4.03 ± 2.07 (0.94–10.82)	**0.01**
CDR	—	1.12 ± 1.17 (0–3)	0.50 ± 0.11 (0–2)[a]	0.74 ± 0.63 (0–2)	**0.03**
CDR-sb	—	5.54 ± 3.75 (1–14)	2.76 ± 2.44 (0–9)[a]	3.44 ± 3.19 (0.5–10.5)	**0.04**
CDR plus NACC FTLD-sb	—	8.34 ± 5.68 (2–18)	5.38 ± 3.29 (2–11.5)	5.86 ± 4.35 (1.5–13.5)	0.29
MMSE	29.03 ± 1.96 (27–30)	23.47 ± 5.67 (6–30)[c]	23.77 ± 5.69 (5–30)[c]	21.73 ± 6.83 (5–30)[c]	**<0.001**
Scanner type (1/2)	44/50	35/29	18/16	14/22	0.44
nfvPPA phenotype (AOS/agrammatic/mixed)	—	—	2/14/18	—	—

Mayo Clinic cohort

	HC-Mayo	bvFTD	nfvPPA	svPPA	p Value
N	15	10	14	18	
Age at MRI, y	61.07 ± 7.75 (51–77)	59.52 ± 9.42 (47.2–75.6)	66.95 ± 7.81 (48.4–77)	62.49 ± 7.77 (44.6–72.8)	0.13
Sex, M/F	5/10	3/7	9/5	10/8	0.91
Education, y	14.4 ± 1.89 (12–18)	14.4 ± 2.07 (12–18)	15.36 ± 3.37 (12–20)	15.56 ± 2.07 (12–20)	0.43
Disease duration, y	—	2.82 ± 1.06 (1.52–4.55)	3.81 ± 2.25 (0.9–8.62)	3.38 ± 1.40 (1.38–5.84)	0.38
MMSE	—	25.44 ± 5.62 (13–29)	28.29 ± 2.61 (22–30)	26.84 ± 2.25 (23–30)	0.15
nfvPPA phenotype (AOS/agrammatic/mixed)	—	—	1/3/10	—	—

Abbreviations: AOS = apraxia of speech; bvFTD = behavioral variant frontotemporal dementia; CDR = Clinical Dementia Rating; CDR plus NACC FTLD = Clinical Dementia Rating plus National Alzheimer Coordinating Center for Frontotemporal Lobar Degeneration sub of boxes; CDR-sb = Clinical Dementia Rating sum of boxes; HCs = healthy controls; MMSE = Mini-Mental State Examination; nfvPPA = nonfluent/agrammatic variant primary progressive aphasia; svPPA = semantic variant primary progressive aphasia.
Values are reported as mean values ± SDs (min-max). The threshold of statistical significance was set at $p < 0.05$. p Values refer to analysis of variance models followed by post hoc, Bonferroni-corrected comparisons or Pearson χ^2, as appropriate.
[a] Statistically significant difference with bvFTD.
[b] Statistically significant difference with svPPA.
[c] Statistically significant difference with HCs.

Research Group at the Mayo Clinic in Rochester, MN, between April 2007 and September 2020 and comprised 42 patients (i.e., 10 bvFTD, 14 nfvPPA, and 18 svPPA) with a diagnosis of frontotemporal lobar degeneration (FTLD), based on either postmortem histopathologic demonstration (n = 17, including 14 nfvPPA and 3 bvFTD) or negative amyloid PET (n = 25, including 18 svPPA and 7 bvFTD) (Table 1). Patients did not present any known genetic variation, similar to the Milan cohort. Fifteen age-matched and sex-matched healthy controls (HC-Mayo) were also selected. Local ethical standards committees on human experimentation approved the study protocols, and all participants provided written informed consent according to the Declaration of Helsinki.

Clinical and Cognitive Assessment

Clinical evaluation was performed by experienced neurologists, recording disease duration at presentation. Global disease severity was assessed using the Clinical Dementia Rating (CDR)[16] and CDR plus National Alzheimer's Coordinating Center FTLD scales.[17] Participants of the Milan cohort also underwent a comprehensive neuropsychological assessment (Table 2). Details of cognitive assessment protocol and speech evaluation have been previously described.[14]

Genetic Testing

The presence of pathologic *C9orf72* expansions and/or known pathogenic genetic variations in the *GRN, MAPT, FUS, TARDBP,*

Table 2 Neuropsychological Features of the Milan Cohort

	HC-old	bvFTD	nfvPPA	svPPA
N	94	64	34	36
Age at MRI, y	65.35 ± 6.39 (51–79)	65.92 ± 7.91 (45–79)	69.01 ± 8.3 (53–83)	66.94 ± 8.34 (48–81)
Sex, M/F	36/58	38/26	12/22	18/18
Education, y	12.51 ± 4.35 (5–24)	9.65 ± 3.53[a] (3–17)	10.06 ± 5.8 (3–22)	11.83 ± 4.68 (3–18)
Global cognition				
MMSE	29.03 ± 1.96 (27–30)	23.47 ± 5.67[a] (6–30)	23.94 ± 5.67[a] (5–30)	21.73 ± 6.83[a] (5–30)
FAB	—	11 ± 4.23 (1–17)	9.7 ± 4.99 (0–16)	12.68 ± 4.63 (0–17)
Memory				
Digit span forward	5.93 ± 1.11 (3–9)	4.85 ± 1.14[a] (3–7)	4.03 ± 0.93[a] (2–6)	4.94 ± 1.46[a] (0–7)
RAVLT delayed	9.5 ± 2.85 (3–14)	2.96 ± 3.18[a,b] (0–11)	6.61 ± 3.77[a] (0–12)	3 ± 3.66[a,b] (0–11)
Corsi block-tapping	5.16 ± 1.15 (2–7)	3.84 ± 1.45 (0–7)	5.46 ± 7.45 (2–40)	4.42 ± 1.23 (2–7)
Attention and executive functions				
Attentive matrices	50.6 ± 7.73 (23–60)	39.47 ± 11.81[a] (10–60)	34.96 ± 14.24[a] (1–58)	40.97 ± 13.49[a] (12–59)
CPM	31.09 ± 4.11 (16–35)	21.61 ± 8.13[a] (0–35)	22.44 ± 7.63[a] (6–34)	24.24 ± 7.91[a] (7–36)
Digit span backward	4.6 ± 1.21 (2–8)	3.44 ± 1.1[a] (0–5)	2.5 ± 1.25[a] (0–4)	3.33 ± 1.44[a] (0–6)
Card sorting test perseverations	4.18 ± 3.79 (0–16)	17.25 ± 14.57[a,c] (0–46)	9.71 ± 10.16 (0–42)	6.33 ± 6.07 (0–21)
Visuospatial abilities				
Rey figure copy	30.5 ± 5.4 (4–36)	22.84 ± 10.32[a] (0–36)	22.67 ± 9.18 (0–35)	29.09 ± 5.25 (16–35)
Language				
AAT (repetition)	—	—	127.83 ± 24.62 (49–148)	142.43 ± 11.24 (120–180)
Token test	33.97 ± 1.74 (29.5–36)	27.47 ± 6.87[a] (5–36)	24.74 ± 6.34[a] (13–35)	22.33 ± 9.54[a] (4–36)
CaGi confrontation naming	—	—	43.12 ± 6.73[c] (22–48)	19.44 ± 12.95[b] (0–47)
CaGi single-word comprehension	—	—	47.55 ± 1.53[c] (41–48)	38.35 ± 9.07[b] (18–48)
Pyramid-palm tree	—	—	46.8 ± 5.66[c] (29–52)	36.35 ± 6.85[b] (25–50)
Fluency				
Phonemic fluency	37.3 ± 9.37 (15–56)	15.02 ± 11.29[a] (0–39)	8.62 ± 7.38[a] (0–25)	15.25 ± 11.1[a] (0–31)
Semantic fluency	44.12 ± 9.62 (12–66)	21.6 ± 10.56[a,c] (0–48)	19.9 ± 11.3[a,c] (0–48)	11.45 ± 8.1[a] (0–28)
Mood and behavior				
NPI	—	28.46 ± 19.35 (3–74)	16.25 ± 18.82 (1–71)	16.23 ± 12.05 (0–44)
BDI	6.86 ± 3.6 (0–12)	—	—	—
FBI total	—	21.23 ± 11.26 (6–46)	14.5 ± 10.37 (5–36)	18 ± 10.7 (6–38)

Abbreviations: AAT = Aachener Aphasie Test; BDI = Beck Depression Inventory; bvFTD = behavioral variant frontotemporal dementia; CPM = Colored Progressive Matrices; CST = Card Sorting Tests; FAB = Frontal Assessment Battery; FBI = Frontal Behavioral Inventory; HCs = healthy controls; MMSE = Mini-Mental State Examination; nfvPPA = nonfluent/agrammatic variant primary progressive aphasia; NPI = Neuropsychiatric Inventory; RAVLT = Rey Auditory Verbal Learning Test; svPPA = semantic variant primary progressive aphasia.

Values are mean values ± SDs (range). *p* Values refer to analysis of variance models, corrected for age, sex, and education, followed by post hoc pairwise comparisons, Bonferroni corrected for multiple comparisons. The threshold of statistical significance was set at $p < 0.05$.

[a] Statistically significant difference with HC.
[b] Statistically significant difference with nfvPPA.
[c] Statistically significant difference with svPPA.

TBK1, TREM2, OPTN, and *VCP* genes was assessed from blood samples using optimized protocols.[18] Carriers of genetic variations were excluded.

MRI Acquisition

Milan Sample

All participants of the Milan cohort underwent brain MRI on a 3T scanner (Philips Medical Systems, Best, the Netherlands) at San Raffaele Hospital. The original scanner was substituted with an upgraded model from the same manufacturer in 2016. Details of MRI acquisition protocols (including at least 3-dimensional [3D] T1-weighted and resting-state fMRI [RS fMRI]) are summarized in eTable 1 (links.lww.com/WNL/ C747). During RS fMRI, individuals were instructed to remain motionless, keeping their eyes closed, and not to think about anything in particular.

Mayo Clinic Sample

Patients and healthy controls of the Mayo Clinic cohort also underwent brain MRI on a 3T scanner (GE Healthcare, Milwaukee, WI) including a 3D T1-weighted MPRAGE sequence (for details of MRI protocol, see eTable 1, links.lww. com/WNL/C747).

MRI Analysis

MRI analysis was performed at the Neuroimaging Research Unit, San Raffaele Hospital in Milan by experienced observers, blinded to participants' identity.

Voxel-Based Morphometry

First, we aimed to identify the disease epicenters of each FTD variant, to be used as seeds for a subsequent SFC analysis. To this purpose, we investigated gray matter (GM) volumetric alterations in the Mayo Clinic patient cohort using voxel-based morphometry (VBM) with SPM12[19] and the DARTEL registration method.[20,21] VBM group comparisons were then tested using analysis of variance (ANOVA) models between each FTD group and controls. The local maximum of the *t* statistics across significant clusters identified the atrophy peaks for each clinical variant. Using the MarsBaR ROI toolbox for SPM12,[22] a spherical 10-mm radius ROI was created around each subgroup's most significant atrophy peak. The choice of using an independent set of patients with FTD with high confidence of FTLD pathology for seed definition was made to avoid circular reasoning when correlating atrophy with SFC data.

SFC Analysis

In brief, SFC is a graph theory–based method that allows to map the connectivity patterns of selected brain seed regions at different step (or "link-step") distances, creating a framework where a step refers to the number of links (edges) that belongs to a path connecting a node to the seed area. In SFC analysis, the degree of stepwise connectivity of a voxel *j* for a given step distance *l* and a seed region *i* is computed from the count of all paths that (1) connect voxel *j* and any voxel in seed region *i* and (2) have an exact length of *l*.[12] Throughout this article, we

will use the term "direct" connections when assessing 1-step functional topological distances (step 1), whereas the term "indirect" will refer to further-step distances from the seed region (steps 2–4). The pipeline adopted for this study (including RS fMRI data preprocessing, functional connectome reconstruction, and calculation of SFC degree) has been recently described.[23] Of note, the number of "steps" merely describes the topological distance between 2 nodes within the brain functional connectome; therefore, it does not refer to the presence of a direct/indirect axonal connection.

For each FTD variant of the Milan cohort, SFC analysis was performed using as seed region the specific ROI previously identified in the Mayo Clinic population. For each group of healthy controls (i.e., HC-old and HC-young), 3 different SFC models were created, one for each ROI. Given the lack of directionality information provided by RS fMRI data, in SFC, we did not include any restrictions about recurrent pathways crossing the seed regions multiple times. All maps across different link-step distances from 1 to 4 were used to describe connectivity differences between HC-old and FTD participants. Further steps were not included in this analysis because SFC patterns became stable for link-step distances above 4.

Subsequently, a combined version of all SFC 1–4 maps into 1 single map from nondisrupted connectivity pathways of HC-young (combined SFC map) was used to investigate the relationships between "standard" healthy neuroimaging patterns and volumetric measures of participants with FTD. To build the SFC combined map, we determined, for each pair of voxels, at which step the relative degree of stepwise connectivity was maximized. Thus, we obtained an SFC combined map for each participant, with values ranging 1 to 4. Finally, the combined SFC map was registered to the 90-region Automated Anatomical Labeling (AAL) atlas to allow correlations with GM volumetric measures of patients with FTD.

## Regional GM Volumetric Measures

Cortical GM maps were obtained from patients with FTD of the Milan cohort using the segmentation step of VBM,[21] while maps of the basal ganglia, hippocampus, and amygdala were obtained using the FMRIB's Integrated Registration and Segmentation Tool in FSL.[24] The AAL atlas was then registered to individual T1-weighted images, masked using the GM maps, by means of linear (FLIRT)[25] and nonlinear (FNIRT)[26] registrations. GM volumes were obtained and multiplied by the normalization factor derived from SIENAx[27] to correct for head size.

Statistical Analysis

Clinical and Cognitive Data

Normal distribution assumption was checked by means of Q-Q plot and Shapiro-Wilks and Kolmogorov-Smirnov tests. Demographic, clinical, and neuropsychological data were compared between groups using age-adjusted, sex-adjusted, and education-adjusted ANOVA models, followed by post

Figure 1 Identification of Disease Epicenters
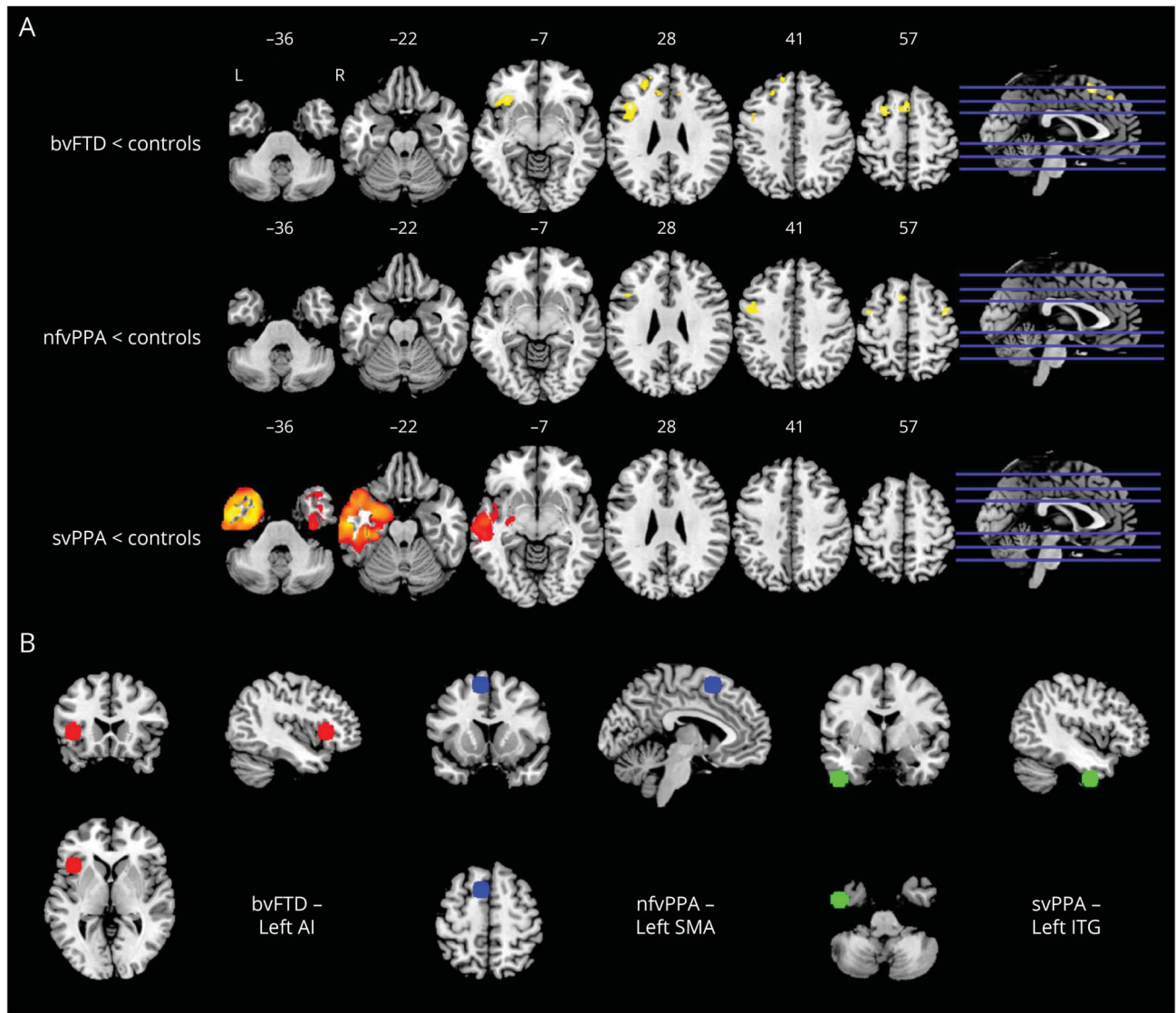
(A) Results of voxel-based morphometry analysis showing regions of significant GM atrophy in patients with FTLD of the Mayo Clinic cohort when compared with healthy controls. Significant clusters are overlaid on the axial sections of the MNI standard brain. Analyses were corrected for age, sex, and total intracranial volume. Statistical threshold for significance was $p < 0.05$, FWE corrected for multiple comparisons. (B) 10-mm radius spheres overlaid on the MNI standard brain show the identified peaks of atrophy. AI = anterior insula; bvFTD = behavioral variant Frontotemporal Dementia; ITG = inferior temporal gyrus; L = left hemisphere; MNI = Montreal Neurological Institute; nfvPPA = nonfluent/agrammatic variant primary progressive aphasia; R = right hemisphere; SMA = supplementary motor area; svPPA = semantic variant primary progressive aphasia.

hoc pairwise comparisons, Bonferroni corrected for multiple comparisons. $p < 0.05$ was set as significance threshold. SPSS Statistics 26.0 software was used.

MRI Data

For the assessment of GM atrophy in the Mayo Clinic cohort, group comparisons were tested using ANOVA model, adjusting for total intracranial volume, age, and sex. Results were assessed at $p < 0.05$ family-wise error (FWE) corrected for multiple comparisons.

For the assessment of SFC in the Milan cohort, voxel-wise analyses were performed using general linear models as implemented in SPM12. Two-sample t test comparisons between controls and each patient group were performed for each of the 4 steps, including age, sex, and scanner type as covariates. Considering that our procedure could lead to non-normal distribution, a threshold-free cluster enhancement method with 5,000 nonparametric permutations, as implemented in the Computational Anatomy Toolbox 12,[28] was used to detect statistically significant differences at $p < 0.05$, FWE corrected.

Correlation Analysis

For each AAL region, correlations between the combined SFC maps obtained in HC-young for each seed ROI and average GM volumes of patients with FTD of the Milan sample were

Figure 2 Stepwise Functional Connectivity Alterations in bvFTD
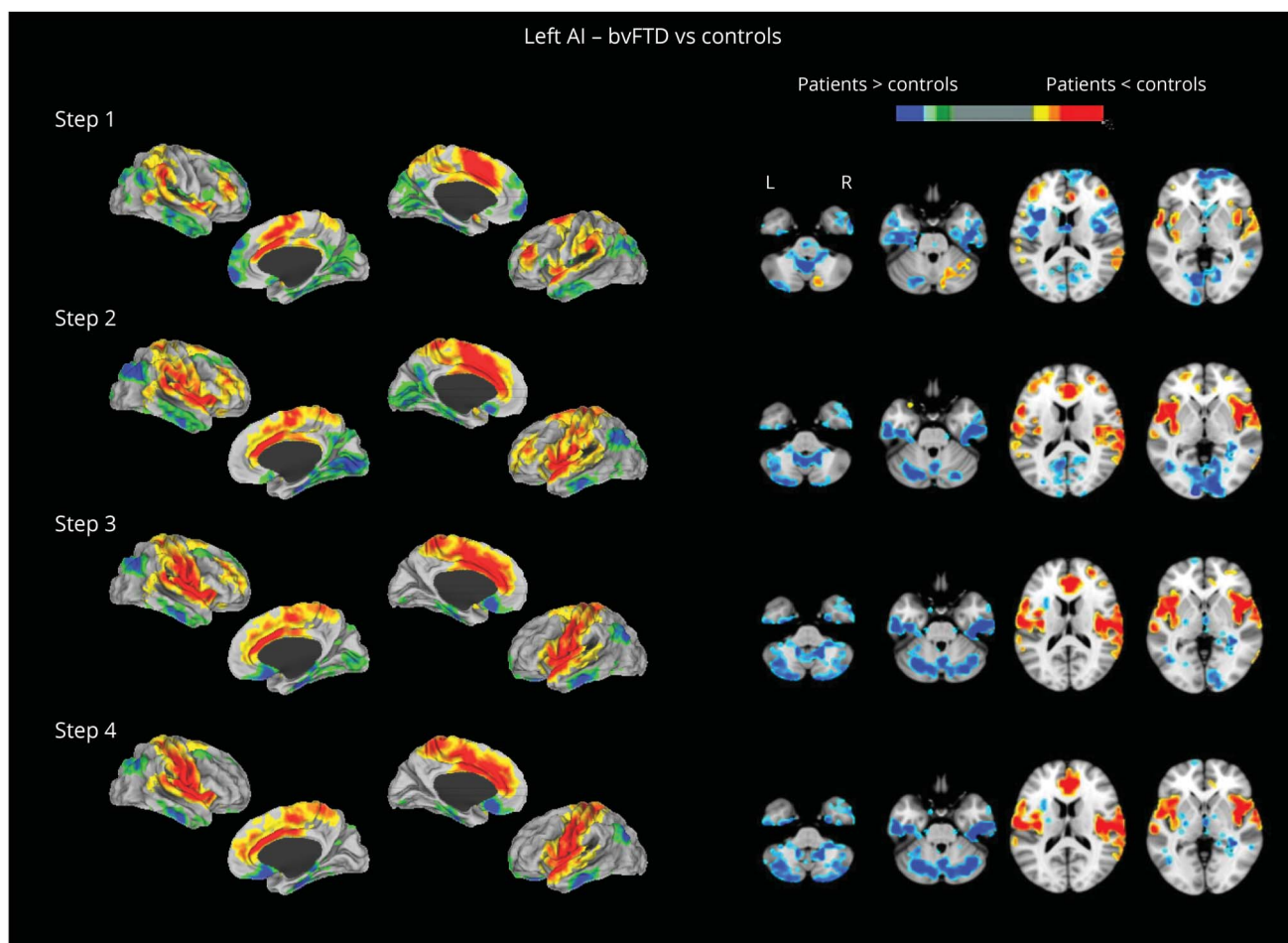
Cortical and subcortical differences between patients with bvFTD and age-matched healthy controls (HC-old) in stepwise functional connectivity of the left AI (red-yellow = lower functional connectivity, blue-green = higher functional connectivity). Statistical threshold for significance was $p < 0.05$, few corrected for multiple comparisons. AI = anterior insula; bvFTD = behavioral variant frontotemporal dementia; L = left hemisphere; R = right hemisphere.

tested using the Spearman correlation coefficient (SPSS Statistics 26.0).

Data Availability

Dataset and codes used for this study will be made available by the corresponding author on request.

Results

Sociodemographic and Clinical Features

All groups were comparable for age, sex, and scanner type (Table 1), although HC-old were more educated than each patient group. FTD subgroups were comparable for education, CDR-FTLD, and MMSE scores. Adjusting for age, sex, and education, significant differences were observed between each FTD group and HC-old regarding measures assessing memory, attention, language, fluency, and executive functions (Table 2). Patients with bvFTD showed additional impairment of visuospatial abilities and worse executive

performance compared with those with svPPA. Patients with svPPA showed significant impairment of confrontation naming, single-word comprehension, and semantic knowledge, compared with those with nfvPPA.

Identification of Disease Epicenters

Disease epicenters of each FTD variant were obtained from the independent (Mayo Clinic) cohort (Figure 1A, eTable 2, links.lww.com/WNL/C747), defined on the following atrophy peaks: the left anterior insula (AI) (MNI coordinates = −40; 20; 3) for bvFTD; the left supplementary motor area (SMA) (−8; 12; 58) for nfvPPA; and the anterior left inferior temporal gyrus (ITG) (−46; −4; −42) for svPPA (Figure 1B).

SFC Analysis

The variant-specific ROIs were used as seed regions to create an SFC model for the respective disease subgroup. SFC differences between each patient group and age-matched HC-old were tested for each disease epicenter ($p < 0.05$, few corrected, eTables 3, 4, and 5, links.lww.com/WNL/C747).

Figure 3 Stepwise Functional Connectivity Alterations in nfvPPA
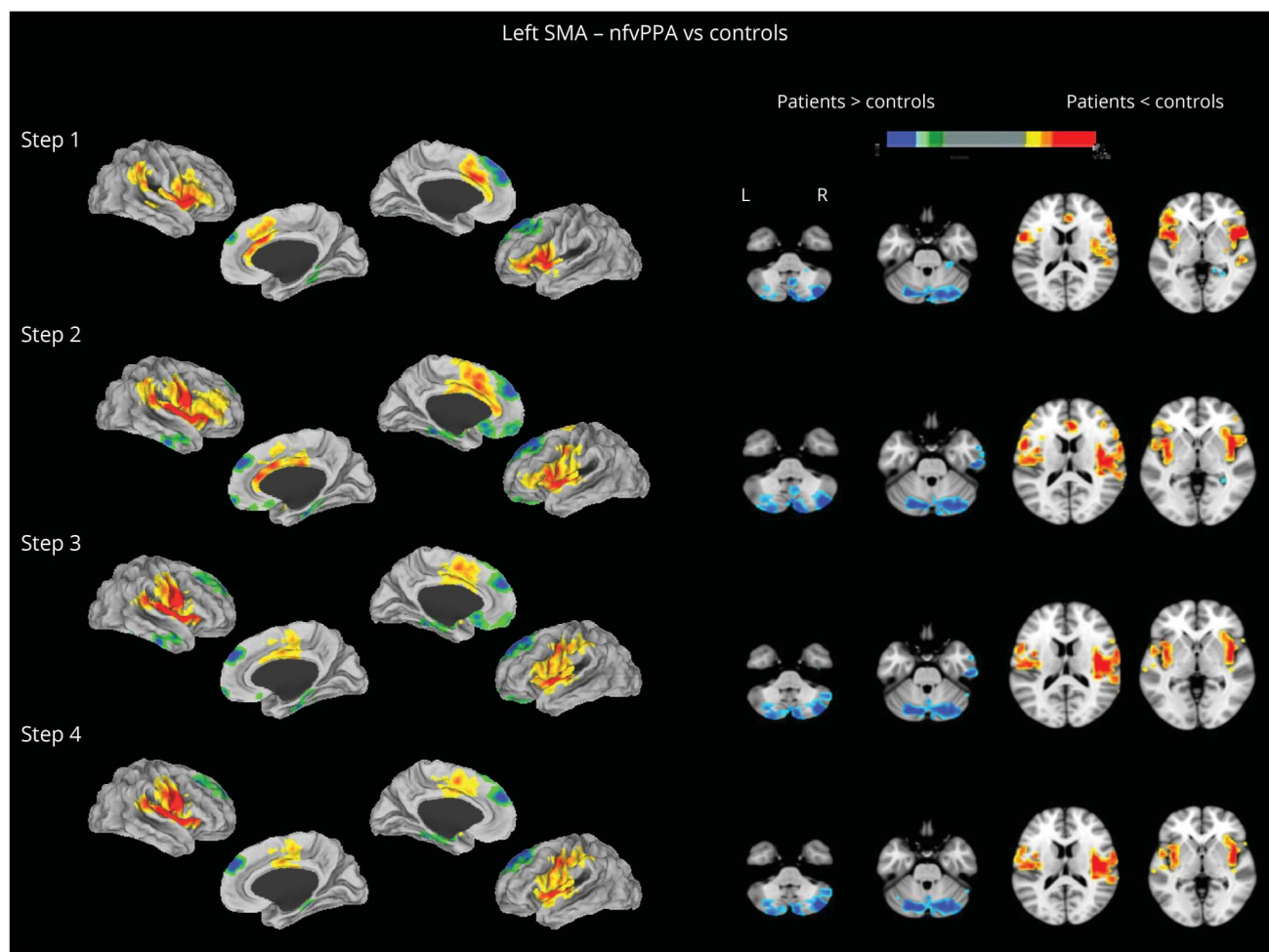
Cortical and subcortical differences between patients with nfvPPA and age-matched healthy controls (HC-old) in stepwise functional connectivity of the left SMA (red-yellow = lower functional connectivity, blue-green = higher functional connectivity). Statistical threshold for significance was $p < 0.05$, FWE corrected for multiple comparisons. FWE = family-wise error; L = left hemisphere; nfvPPA = nonfluent/agrammatic variant primary progressive aphasia; R = right hemisphere; SMA = supplementary motor area.

bvFTD

At 1 link-step distance (i.e., direct connections), the seed ROI placed in the left AI of patients with bvFTD showed reduced functional connectivity (step 1, yellow-red in Figure 2) with bilateral posterior insular, frontal (SMA, paracentral lobule, middle frontal gyrus, and inferior frontal gyrus pars opercularis), parietal (supramarginal gyrus and precuneus), superior temporal, and (mostly anterior) cingulate regions, the posterior right middle temporal gyrus, and right cerebellar regions (crus I–II and lobules VI–VIIIa and VIIIb). By contrast, the left AI showed increased direct connectivity (step 1, blue-green in Figure 2) with its surrounding voxels and the homologous cortex in the right AI, bilateral parietal (inferior parietal lobule), occipital (cuneus, pericalcarine), frontal (superior and inferior frontal gyri), and temporal (inferior and middle temporal, fusiform) regions, the caudate nuclei (with a left-sided prevalence), and left cerebellar regions (crus II, lobules VI–VIIb). When considering indirect connections (steps 2–4), the left AI of patients with bvFTD showed

decreased functional connectivity with the same widespread fronto-temporo-parietal regions as in step 1, with the additional involvement of precentral and postcentral gyri and the insula, bilaterally. Increased indirect connectivity was found with diffuse parietal and occipital cortical regions, with the additional involvement of the orbitofrontal cortices, right middle frontal gyrus, left putamen, and posterior cerebellum. At longer link-step distances, increased connectivity within the AI was absent (step 2) or localized to a small left hemispheric region (steps 3–4).

nfvPPA

At 1 link-step distance, the ROI placed in the left SMA of patients with nfvPPA showed reduced connectivity (Figure 3) with the inferior frontal (pars opercularis/triangularis), lateral precentral, AI, paracentral, and rostral anterior cingulate cortex, bilaterally, and the right supramarginal gyrus. Patients with nfvPPA also showed increased direct connectivity of the left SMA with the surrounding
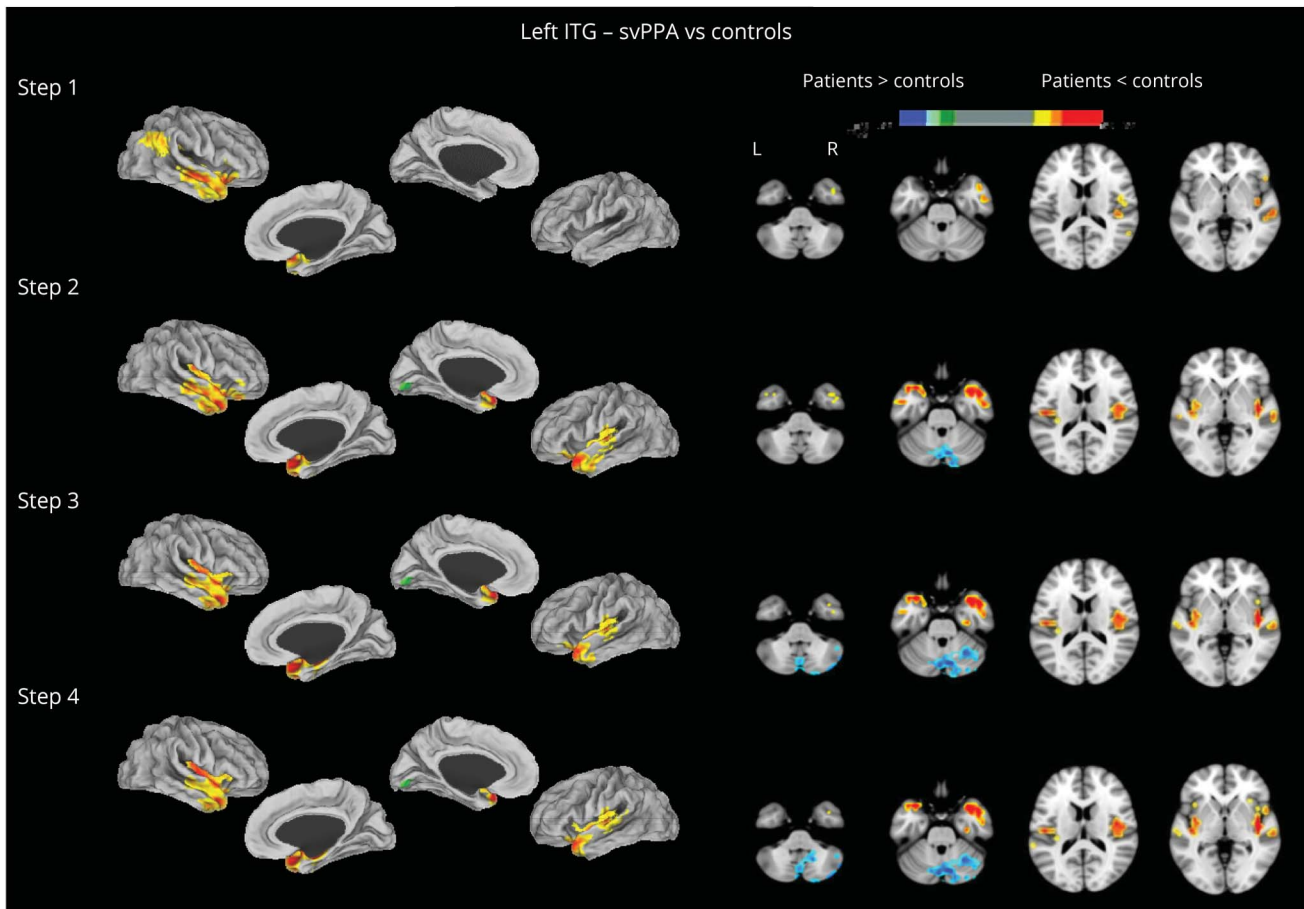
Cortical and subcortical differences between patients with svPPA and healthy controls (HC-old) in stepwise functional connectivity of the left ITG (red-yellow = lower functional connectivity, blue-green = higher functional connectivity). Statistical threshold for significance was $p < 0.05$, FWE corrected for multiple comparisons. FWE = family-wise error; ITG = inferior temporal gyrus; L = left hemisphere; R = right hemisphere; svPPA = semantic variant primary progressive aphasia.

superior frontal and homologous contralateral regions, left lateral middle frontal and right superior frontal, lingual, fusiform, and parahippocampal gyri. At steps 2–4, decreased connectivity involved the same regions as step 1, with the additional involvement of the whole precentral, postcentral, anterior cingulate, and insular cortex, bilaterally. The left SMA of nfvPPA also showed increased indirect connectivity (steps 2–4) with diffuse superior frontal and inferior temporal regions, bilaterally. Across all link steps, patients with nfvPPA showed increased connectivity of the left SMA with cerebellar crus I and lobule VI.

svPPA

At 1 link-step distance, the ROI placed in the left ITG of patients with svPPA showed reduced connectivity (Figure 4) with regions of the right hemisphere, including the anterior portions of the superior, middle, and inferior temporal gyri, insula, and inferior parietal lobule. No areas of increased direct connectivity were identified in svPPA. When considering indirect connections (steps 2–4), patients with svPPA showed decreased connectivity of the left ITG with the bilateral anterior temporal and insular regions, which remained stable at

increasing steps. Regions with increased indirect connectivity of the left ITG in svPPA were found in the left lingual gyrus, cerebellar vermis, and bilateral posterior cerebellum (crus I–II, lobules V–VI). A sensitivity analysis further corrected for the number of contrasts ($p < 0.004$, FWE corrected, eFigures 1–3, links.lww.com/WNL/C747) showed that results were still significant using this very conservative threshold across FTD groups.

Correlations Between Atrophy and SFC Measures

The variant-specific ROIs were also used to create 3 different SFC models in the HC-young group, as represented in Figure 5. For each AAL region, a correlation was found between the average link-step distance from the left ITG in HC-young and the mean GM volume in patients with svPPA ($r = 0.29$, $p = 0.03$, eFigures 4 and 5, links.lww.com/WNL/C747). No significant correlations were found between functional link-step distance from the left AI and the regional mean GM volumes in patients with bvFTD ($r = 0.10$, $p = 0.35$) nor between link-step distance from the left SMA and GM volumes in those with nfvPPA ($r = 0.08$, $p = 0.47$).

Figure 5 SFC Architecture From Disease Epicenters in Healthy Conditions
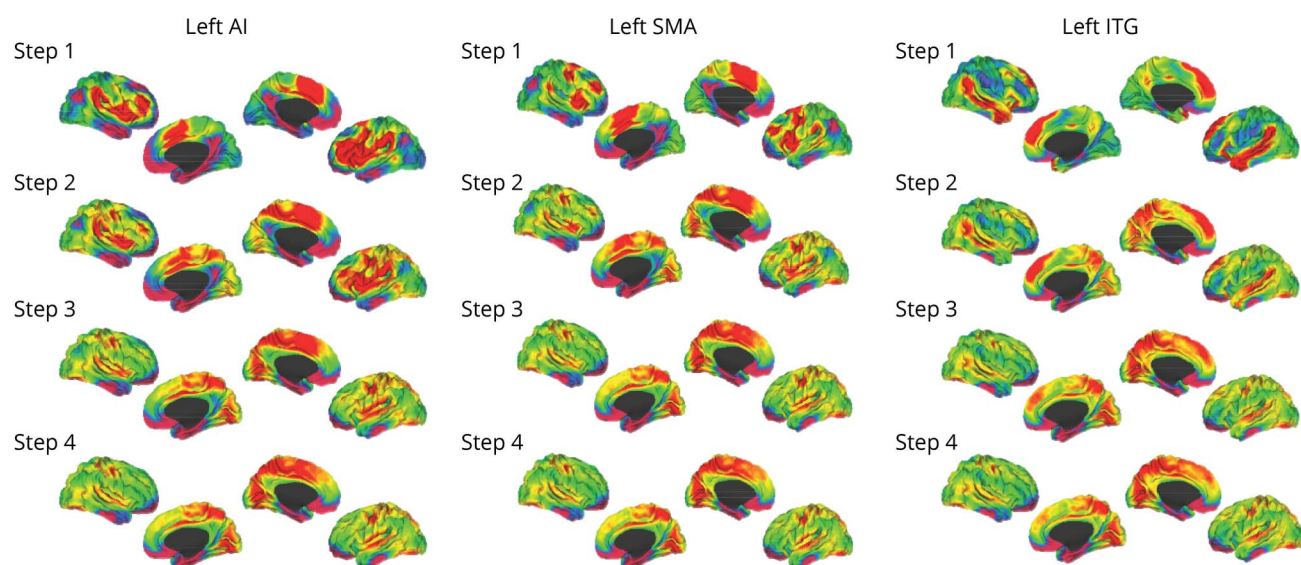
Average stepwise functional connectivity maps in young healthy controls (HC-young) using each seed ROI. Results are depicted in surface space. Red-yellow indicates high strength of connectivity; blue-violet indicates low strength of connectivity. AI = anterior insula; ITG = inferior temporal gyrus; ROI = region of interest; SFC = stepwise functional connectivity; SMA = supplementary motor area.

Discussion

In this study, we explored the pattern of disruption of functional connectivity at increasing topological distance from the disease epicenters of FTD clinical variants, using up-to-date neuroimaging techniques. SFC analysis is a graph theory–based neuroimaging method that detects functional couplings of a selected ROI with other brain regions, at increasing levels of link-step distances. Selecting the peaks of atrophy of an independent cohort of patients with high confidence of FTLD pathology as the seed ROIs for a subsequent whole-brain SFC analyses, we showed extensive reductions of functional connectivity in brain regions with direct and indirect connections with the respective seed regions in the 3 main clinical FTD variants. Patients with FTD also showed more localized connectivity increases involving either short-range direct connections (i.e., 1 step-link distance) or more distant indirect connections (i.e., 2–4 step-link distance). For svPPA, we demonstrated a relationship between the healthy SFC architecture from the disease epicenter and the regional distribution of atrophy in patients. These findings provide evidence supporting the notion of FTD variants as "disconnection syndromes," opening promising perspectives to understand disease progression through brain networks.

The identification of the insula, left SMA, and left anterior temporal lobe as the brain regions with the greatest accumulation of neurodegeneration for bvFTD, nfvPPA, and svPPA, respectively, matches the findings reported in a recent MRI volumetric study.[29] The identification of SMA as the peak of atrophy in nfvPPA was not surprising because the inferior frontal and precentral gyri also showed significant atrophy,

consistent with the mostly mixed (i.e., apraxia of speech plus agrammatic) clinical presentation of these patients.[30] The atrophy patterns also broadly mirror current imaging supporting criteria for the diagnosis of FTD variants,[1,2] consistent with an accurate selection of our sample. Based on such highly replicated observations, we have therefore identified our atrophy peaks as the "disease epicenters" of each variant.[7,31] However, in this study, we used a novel approach in the context of FTD, combining structural data with RS fMRI in an innovative way. In fact, SFC does not simply describe alterations of functional connectivity on a whole-brain scale, but also discriminates between the involvement of 1-step (direct) and further-step distance (indirect) connections, therefore allowing to discriminate between upstream and downstream consequences of neurodegeneration in the disease epicenters, which might be misinterpreted by more traditional approaches.

In bvFTD, we observed significant decrease of functional connectivity in widespread brain regions that were directly connected with the left AI. The substantial decrease of functional connectivity between the AI and the anterior cingulate cortex was consistent with the known primary damage of the salience network in this clinical presentation.[32,33] Decreased connectivity of the AI with widespread frontal regions, including the middle frontal and supplementary motor regions, supports the notion that fronto-insular decoupling may cause executive, attentional, and goal-oriented motor planning deficits.[32,34] Decreased AI functional connectivity with a key posterior associative region such as the precuneus—a central component of the default mode network— supports the hypothesis that the previously observed within-network hyperconnectivity of the default mode network[33,35] might be a direct

consequence of functional disconnection of posterior brain regions from the frontal hubs. Similarly, decreased direct functional connectivity with the posterior insula and the closely related parietal somatosensory association cortex (involved in the cortical elaboration of interoceptive and nociceptive stimuli)[36] might be due to loss of integration from the AI, which is involved instead in emotional salience and cognitive control and presents different cytoarchitectural features and structural connections.[32,37] Our findings of decreased 1-step connectivity throughout these regions, although in line with previous fMRI reports, deepen current knowledge about such alterations, demonstrating that they are due to the involvement of the most direct functional connections with the disease epicenter, suggesting their role as an early pathogenic marker of bvFTD. At increasing link-step distances from the AI (i.e., indirect connections), decreased functional connectivity became even more widespread, with greater functional disconnection with frontal, insular, and cingulate regions and involvement of the sensorimotor regions—unaffected in step 1—supporting the hypothesis that the failure of functional integrity observed in bvFTD[9,11,38] might result from widespread downstream propagation effects of neurodegeneration from the disease epicenter.

In addition, when examining the results obtained in patients with nfvPPA and svPPA, we demonstrated predominantly reduced functional connectivity of the respective seed regions with directly connected cortical regions, including bilateral inferior frontal opercular regions (key regions of the speech production network[10]) in nfvPPA and the contralateral anterior temporal lobe (part of the semantic functional network[39]) in svPPA. Decreased connectivity through 1-step connections with right hemispheric cortical regions was evident in both PPA variants and particularly striking in the case of svPPA. Consistent with the fact that both these linguistic networks are bilaterally represented,[10,39] our SFC analysis suggests that direct interhemispheric connections are significantly affected in the linguistic presentations of FTD, mostly in svPPA—the variant showing a greater bilateral atrophy distribution.[40] Similar to bvFTD, although to a lesser extent, we found further evolution of decreased connectivity through indirect connections at increasing step-link distances from the respective seed regions, involving more diffuse fronto-opercular regions in nfvPPA and bilateral anterior temporal regions in svPPA (because, in this case, SFC disruption patterns apparently "bounced back" to the left hemispheric disease epicenter). Therefore, also for PPA variants, SFC was able to delineate patterns of functional decoupling of disease epicenters with brain regions showing direct or indirect connections, possibly through the frontal aslant tract and the dorsal frontoparietal language pathway for nfvPPA[10,41,42] or the interhemispheric fibers of the anterior commissure mediating integration of multimodal semantic knowledge in the case of svPPA,[8,43] expanding previous evidence in the neuroimaging field.[8,10,41]

In patients with bvFTD and nfvPPA, SFC was also able to detect increased connectivity of the respective disease epicenters with regions at 1-link steps, either with maximal physical proximity in the surrounding areas or within the homologous contralateral cortices. Moreover, bvFTD also showed increased direct connectivity with widespread long-range connected regions; namely, bvFTD showed increased direct functional connectivity of the left AI with the surrounding voxels, the contralateral AI (structurally connected through transcallosal fibers), the caudate nuclei (through insulo-striatal fibers),[44] the orbitofrontal and parieto-occipital cortices (interconnected by the inferior fronto-occipital fasciculus, which receives fiber contributions from the AI),[45] the inferior temporal cortices (through the uncinate fasciculus),[45] and the ipsilateral posterior cerebellum (through cerebro-cerebellar circuits)[46]; whereas nfvPPA showed increased connectivity of the left SMA with the surrounding and—to a lesser extent—homologous contralateral cortical regions. Such pattern of both short-range (common to bvFTD and nfvPPA) and long-range increased direct connectivity (in this study, observed mostly for bvFTD) might be compatible with a loss of local interneuronal and, at the same time, with a more complex and widespread mechanism of functional rearrangements. This was not the first RS fMRI study showing increased local connectivity within the prefrontal and parieto-occipital cortices of patients with FTD.[33,35,47] However, SFC analysis allowed us to draw a more complex picture of the interaction between 3 phenomena, namely: (1) the widespread patterns of long-range decreased connectivity within regions of the salience network, across both direct and indirect connections; (2) short-range increased connectivity, mostly evident when assessing direct connections; and (3) long-range increased connectivity, progressively apparent from direct to indirect connections. Based on our observations in bvFTD, we speculate that the relationship between—at least—the former 2 phenomena might be more compatible with a maladaptive process, whereas the long-range increased connectivity might also play a role to partially compensate for neurodegeneration, although we could not provide within the cross-sectional design of our study unconfutable evidence pointing toward this suggestion. We also suggest a similar interplay between locally increased direct connectivity and longer-range functional disconnection in the context of nfvPPA, although such findings need replication in larger cohorts.

Increased functional connectivity was also found in regions at greater link-step distances for all patient groups. Of note, increased connectivity with the posterior cerebellar regions (e.g., crus and lobule VI) was found across patients with bvFTD, nfvPPA, and svPPA. This is consistent with the physiologic role of these cognitive/affective regions of the posterior cerebellum (involved in the modulation of emotions and social behavior)[48] and the few previous fMRI reports reporting disrupted functional connectivity of cerebellar regions in FTD.[47,49] Although the role in cognition and the topological organization of the cerebellar cortex has started being elucidated only recently,[48] this is an exciting area of developing research to understand FTD pathophysiology.

Another important aim of this study was to test the relationship between healthy brain SFC architecture and the distribution of atrophy in each FTD variant because the identification of determinants of pathologic progression from the epicenters has a clear relevance for modeling disease evolution. We provided evidence of a significant—although weak—correlation between SFC architecture propagating from the left ITG and the distribution of atrophy in svPPA. This finding is consistent with recent evidence of a striking resemblance between the large-scale functional network propagating from the left temporal pole and atrophy patterns in an independent sample of patients with svPPA,[8] supporting the hypothesis that pathologic propagation in FTD might be due to a transsynaptic or transneuronal spreading mediated by the complex, highly structured topology of neural networks,[6,50] as recently shown also for Alzheimer disease[51] and Parkinson disease.[52] However, we could not replicate this finding in patients with bvFTD and nfvPPA. We hypothesize that the more severe and, overall, discretely localized pattern of atrophy, together with the relatively longer disease duration characterizing patients with svPPA, might have driven, in this variant only, the significance of such correlation, which would need larger samples and a longitudinal study design to be definitively demonstrated also in other FTD variants.

Our study has some caveats and limitations. First, our cross-sectional design did not allow to draw strong conclusions regarding the evolution of observed increased/decreased connectivity, its maladaptive or compensatory role, nor its relationship with disease worsening and atrophy distribution. In addition, SFC does not allow to make straightforward inference on the neuroanatomical underpinnings of direct/indirect connectivity because "steps" are mathematical constructs that do not necessarily correlate with mono/polysynaptic connections. As a technical constraint, we needed to establish an intermediate size of 10 mm radius for seed ROIs to make a balance between region specificity and functional matrix dimensions. For this reason, we could not discriminate SFC rearrangements between dorsal and ventral anterior insular regions, which display different brain structural connections.[32,37] Moreover, we could not eliminate a significant difference in education levels between controls and patients with bvFTD of the Milan cohort—although correcting for this variable, and for some patients of the Mayo Clinic cohort (e.g., svPPA), amyloid-PET negativity was used to support high confidence of FTLD pathology, in the absence of actual postmortem confirmation. Finally, as noted earlier, we failed to detect a significant correlation between whole-brain SFC architecture of controls and atrophy distribution in bvFTD and nfvPPA.

Nonetheless, we fulfilled the main aim of our study, which was to propose SFC analysis as a new approach for the assessment of brain network disruption in patients affected by FTD disorders, both through direct and indirect connections. Our findings revealed novel insights regarding the topology of functional disconnection across FTD syndromes, showing which rearrangements are related most directly with brain atrophy, holding the promise to provide optimized predictive models of disease progression in future longitudinal studies.

Disclosure
F. Agosta is an Associate Editor of *NeuroImage: Clinical*, has received speaker honoraria from Biogen Idec, Roche, and Zambon, and receives or has received research supports from the Italian Ministry of Health, AriSLA (Fondazione Italiana di Ricerca per la SLA), the European Research Council, and Foundation Research on Alzheimer Disease. E.G. Spinelli, S. Basaia, C. Cividini, F. Falbo, C. Pavone, and N. Riva have nothing to disclose. E. Canu has received research supports form the Italian Ministry of Health. V. Castelnovo, G. Magnani, F. Caso, P. Caroppo, S. Prioni, C. Villa, L. Tremolizzo, and I. Appollonio have nothing to disclose. V. Silani received compensation for consulting services and/or speaking activities from AveXis, Cytokinetics, Italfarmaco, and Zambon, and receives or has received research supports form the Italian Ministry of Health, AriSLA, and E-Rare Joint Transnational Call. K.A. Josephs receives support from the US National Institute of Health. J.L. Whitwell receives support from the US National Institute of Health. M. Filippi is Editor-in-Chief of the *Journal of Neurology*, Associate Editor of *Human Brain Mapping*, Associate Editor of *Radiology*, and Associate Editor of *Neurological Sciences* and has received compensation for consulting services from Alexion, Almirall, Biogen, Merck, Novartis, Roche, and Sanofi; speaking activities from Bayer, Biogen, Celgene, Chiesi Italia SpA, Eli Lilly, Genzyme, Janssen, Merck-Serono, Neopharmed Gentili, Novartis, Novo Nordisk, Roche, Sanofi, Takeda, and TEVA; participation in Advisory Boards for Alexion, Biogen, Bristol-Myers Squibb, Merck, Novartis, Roche, Sanofi, Sanofi-Aventis, Sanofi-Genzyme, and Takeda; and scientific direction of educational events for Biogen, Merck, Roche, Celgene, Bristol-Myers Squibb, Lilly, Novartis, and Sanofi-Genzyme; he receives research support from Biogen Idec, Merck-Serono, Novartis, Roche, Italian Ministry of Health, and Fondazione Italiana Sclerosi Multipla. Go to Neurology.org/N for full disclosures.

Appendix Authors

Name	Location	Contribution
Federica Agosta, MD, PhD	IRCCS San Raffaele Scientific Institute, and Vita-Salute San Raffaele University, Milan, Italy	Study concept, analysis, and interpretation of data; drafting/revising the article; study supervision
Edoardo Gioele Spinelli, MD, PhD	IRCCS San Raffaele Scientific Institute, Milan, Italy	Drafting/revision of the article for content; major role in the acquisition of data; analysis and interpretation of data; and statistical analysis
Silvia Basaia, PhD	IRCCS San Raffaele Scientific Institute, Milan, Italy	Drafting/revision of the article for content; major role in the acquisition of data; analysis and interpretation of data; and statistical analysis
Camilla Cividini, MSc	IRCCS San Raffaele Scientific Institute, Milan, Italy	Drafting/revision of the article for content; analysis of data
Francesco Falbo, MD	IRCCS San Raffaele Scientific Institute, and Vita-Salute San Raffaele University, Milan, Italy	Drafting/revision of the article for content; acquisition and analysis of data
Costanza Pavone, MD	IRCCS San Raffaele Scientific Institute, and Vita-Salute San Raffaele University, Milan, Italy	Drafting/revision of the article for content; acquisition and analysis of data
Nilo Riva, MD, PhD	IRCCS San Raffaele Scientific Institute, Milan, Italy	Revision of the article for content; acquisition and analysis of data
Elisa Canu, MSc, PhD	IRCCS San Raffaele Scientific Institute, Milan, Italy	Revision of the article for content; acquisition of data; interpretation of data
Veronica Castelnovo, MSc, PhD	IRCCS San Raffaele Scientific Institute, Milan, Italy	Drafting/revision of the article for content; acquisition and analysis of data
Giuseppe Magnani, MD	IRCCS San Raffaele Scientific Institute, Milan, Italy	Revision of the article for content; acquisition of data
Francesca Caso, MD, PhD	IRCCS San Raffaele Scientific Institute, Milan, Italy	Revision of the article for content; acquisition of data
Paola Caroppo, MD, PhD	Fondazione IRCCS Istituto Neurologico Carlo Besta, Milan, Italy	Revision of the article for content; acquisition and analysis of data
Sara Prioni, MSc	Fondazione IRCCS Istituto Neurologico Carlo Besta, Milan, Italy	Revision of the article for content; acquisition and analysis of data
Cristina Villa, PhD	Fondazione IRCCS Istituto Neurologico Carlo Besta, Milan, Italy	Revision of the article for content; acquisition and analysis of data
Lucio Tremolizzo, MD	"San Gerardo" Hospital and University of Milano-Bicocca, Monza, Italy	Revision of the article for content; acquisition and analysis of data
Ildebrando Appollonio, MD	"San Gerardo" Hospital and University of Milano-Bicocca, Monza, Italy	Revision of the article for content; acquisition and analysis of data

Appendix (continued)

Name	Location	Contribution
Vincenzo Silani, MD	IRCCS Istituto Auxologico Italiano, and Università degli Studi di Milano, Italy	Revision of the article for content; acquisition and analysis of data
Keith A. Josephs, MD, MST, MSc	Mayo Clinic, Rochester, MN	Drafting/revision of the article for content; major role in the acquisition of data; study concept and design; and interpretation of data
Jennifer L. Whitwell, PhD	Mayo Clinic, Rochester, MN	Drafting/revision of the article for content; major role in the acquisition of data; study concept and design; and interpretation of data
Massimo Filippi, MD	IRCCS San Raffaele Scientific Institute, and Vita-Salute San Raffaele University, Milan, Italy	Study concept and interpretation of data; revising the article; study supervision

References

1. Rascovsky K, Hodges JR, Knopman D, et al. Sensitivity of revised diagnostic criteria for the behavioural variant of frontotemporal dementia. *Brain.* 2011;134(pt 9):2456-2477.
2. Gorno-Tempini ML, Hillis AE, Weintraub S, et al. Classification of primary progressive aphasia and its variants. *Neurology.* 2011;76(11):1006-1014.
3. Warren JD, Rohrer JD, Hardy J. Disintegrating brain networks: from syndromes to molecular nexopathies. *Neuron.* 2012;73(6):1060-1062.
4. Zuo XN, Ehmke R, Mennes M, et al. Network centrality in the human functional connectome. *Cereb Cortex.* 2012;22(8):1862-1875.
5. van den Heuvel MP, Sporns O. Network hubs in the human brain. *Trends Cogn Sci.* 2013;17(12):683-696.
6. Seeley WW, Crawford RK, Zhou J, Miller BL, Greicius MD. Neurodegenerative diseases target large-scale human brain networks. *Neuron.* 2009;62(1):42-52.
7. Zhou J, Gennatas ED, Kramer JH, Miller BL, Seeley WW. Predicting regional neurodegeneration from the healthy brain functional connectome. *Neuron.* 2012;73(6):1216-1227.
8. Collins JA, Montal V, Hochberg D, et al. Focal temporal pole atrophy and network degeneration in semantic variant primary progressive aphasia. *Brain.* 2017;140(2):457-471.
9. Filippi M, Basaia S, Canu E, et al. Brain network connectivity differs in early-onset neurodegenerative dementia. *Neurology.* 2017;89(17):1764-1772.
10. Mandelli ML, Welch AE, Vilaplana E, et al. Altered topology of the functional speech production network in non-fluent/agrammatic variant of PPA. *Cortex.* 2018;108:252-264.
11. Reyes P, Ortega-Merchan MP, Rueda A, et al. Functional connectivity changes in behavioral, semantic, and nonfluent variants of frontotemporal dementia. *Behav Neurol.* 2018;2018:9684129.
12. Sepulcre J, Sabuncu MR, Yeo TB, Liu H, Johnson KA. Stepwise connectivity of the modal cortex reveals the multimodal organization of the human brain. *J Neurosci.* 2012;32(31):10649-10661.
13. Costumero V, d'Oleire Uquillas F, Diez I, et al. Distance disintegration delineates the brain connectivity failure of Alzheimer's disease. *Neurobiol Aging.* 2020;88:51-60.
14. Agosta F, Ferraro PM, Canu E, et al. Differentiation between subtypes of primary progressive aphasia by using cortical thickness and diffusion-tensor MR imaging measures. *Radiology.* 2015;276(1):219-227.
15. Folstein MF, Folstein SE, McHugh PR. "Mini-mental state." A practical method for grading the cognitive state of patients for the clinician. *J Psychiatr Res.* 1975;12(3):189-198.
16. Morris JC. The Clinical Dementia Rating (CDR): current version and scoring rules. *Neurology.* 1993;43(11):2412-2414.
17. Knopman DS, Kramer JH, Boeve BF, et al. Development of methodology for conducting clinical trials in frontotemporal lobar degeneration. *Brain.* 2008;131(pt 11):2957-2968.
18. Spinelli EG, Ghirelli A, Basaia S, et al. Structural MRI signatures in genetic presentations of the frontotemporal dementia/motor neuron disease spectrum. *Neurology.* 2021;97(16):e1594-e1607.
19. Statistical Parametric Mapping. Accessed April 26, 2023. fil.ion.ucl.ac.uk/spm/.
20. Ashburner J. A fast diffeomorphic image registration algorithm. *Neuroimage.* 2007;38(1):95-113.
21. Agosta F, Spinelli EG, Riva N, et al. Survival prediction models in motor neuron disease. *Eur J Neurol.* 2019;26(9):1143-1152.
22. MarsBaR region of interest toolbox for SPM. Accessed April 26, 2023. marsbar.sourceforge.net.
23. Basaia S, Agosta F, Diez I, et al. Neurogenetic traits outline vulnerability to cortical disruption in Parkinson's disease. *Neuroimage Clin.* 2022;33:102941.

24. Integrated Registration and Segmentation Tool in FSL. Accessed April 26, 2023. fmrib. ox.ac.uk/fsl/first/index.html.

25. Jenkinson M, Bannister P, Brady M, Smith S. Improved optimization for the robust and accurate linear registration and motion correction of brain images. *Neuroimage*. 2002;17(2):825-841.

26. Andersson J, Jenkinson M, Smith S. *FMRIB Technical Report TR07JA2*. FMRIB Analysis Group of the University of Oxford; 2007.

27. Sienax in FSL. Accessed April 26, 2023. fmrib.ox.ac.uk/fsl/sienax/index.html.

28. Computational Anatomy Toolbox 12. Accessed April 26, 2023. neuro.uni-jena.de/cat/.

29. Bejanin A, Tammewar G, Marx G, et al. Longitudinal structural and metabolic changes in frontotemporal dementia. *Neurology*. 2020;95(2):e140-e154.

30. Canu E, Agosta F, Battistella G, et al. Speech production differences in English and Italian speakers with nonfluent variant PPA. *Neurology*. 2020;94(10):e1062-e1072.

31. Mutlu J, Landeau B, Gaubert M, de La Sayette V, Desgranges B, Chetelat G. Distinct influence of specific versus global connectivity on the different Alzheimer's disease biomarkers. *Brain*. 2017;140(12):3317-3328.

32. Benarroch EE. Insular cortex: functional complexity and clinical correlations. *Neurology*. 2019;93(21):932-938.

33. Seeley WW, Menon V, Schatzberg AF, et al. Dissociable intrinsic connectivity networks for salience processing and executive control. *J Neurosci*. 2007;27(9):2349-2356.

34. Menon V, Uddin LQ. Saliency, switching, attention and control: a network model of insula function. *Brain Struct Funct*. 2010;214(5-6):655-667.

35. Zhou J, Greicius MD, Gennatas ED, et al. Divergent network connectivity changes in behavioural variant frontotemporal dementia and Alzheimer's disease. *Brain*. 2010; 133(pt 5):1352-1367.

36. Aguilar-Rivera M, Kim S, Coleman TP, Maldonado PE, Torrealba F. Interoceptive insular cortex participates in sensory processing of gastrointestinal malaise and associated behaviors. *Sci Rep*. 2020;10(1):21642.

37. Cloutman LL, Binney RJ, Drakesmith M, Parker GJ, Lambon Ralph MA. The variation of function across the human insula mirrors its patterns of structural connectivity: evidence from in vivo probabilistic tractography. *Neuroimage*. 2012;59(4): 3514-3521.

38. Agosta F, Sala S, Valsasina P, et al. Brain network connectivity assessed using graph theory in frontotemporal dementia. *Neurology*. 2013;81(2):134-143.

39. Battistella G, Henry M, Gesierich B, et al. Differential intrinsic functional connectivity changes in semantic variant primary progressive aphasia. *Neuroimage Clin*. 2019;22: 101797.

40. Montembeault M, Brambati SM, Gorno-Tempini ML, Migliaccio R. Clinical, anatomical, and pathological features in the three variants of primary progressive aphasia: a review. *Front Neurol*. 2018;9:692.

41. Bonakdarpour B, Hurley RS, Wang AR, et al. Perturbations of language network connectivity in primary progressive aphasia. *Cortex*. 2019;121:468-480.

42. Mandelli ML, Caverzasi E, Binney RJ, et al. Frontal white matter tracts sustaining speech production in primary progressive aphasia. *J Neurosci*. 2014;34(29): 9754-9767.

43. Catani M, Thiebaut de Schotten M. A diffusion tensor imaging tractography atlas for virtual in vivo dissections. *Cortex*. 2008;44(8):1105-1132.

44. Ghaziri J, Tucholka A, Girard G, et al. Subcortical structural connectivity of insular subregions. *Sci Rep*. 2018;8(1):8596.

45. Nomi JS, Schettini E, Broce I, Dick AS, Uddin LQ. Structural connections of functionally defined human insular subdivisions. *Cereb Cortex*. 2018;28(10):3445-3456.

46. Strick PL, Dum RP, Fiez JA. Cerebellum and nonmotor function. *Annu Rev Neurosci*. 2009;32(1):413-434.

47. Farb NA, Grady CL, Strother S, et al. Abnormal network connectivity in frontotemporal dementia: evidence for prefrontal isolation. *Cortex*. 2013;49(7):1856-1873.

48. Stoodley CJ, Schmahmann JD. Evidence for topographic organization in the cerebellum of motor control versus cognitive and affective processing. *Cortex*. 2010;46(7): 831-844.

49. Meijboom R, Steketee RME, de Koning I, et al. Functional connectivity and microstructural white matter changes in phenocopy frontotemporal dementia. *Eur Radiol*. 2017;27(4):1352-1360.

50. Fornito A, Zalesky A, Breakspear M. The connectomics of brain disorders. *Nat Rev Neurosci*. 2015;16(3):159-172.

51. Filippi M, Basaia S, Canu E, et al. Changes in functional and structural brain connectome along the Alzheimer's disease continuum. *Mol Psychiatry*. 2020;25(1): 230-239.

52. Filippi M, Basaia S, Sarasso E, et al. Longitudinal brain connectivity changes and clinical evolution in Parkinson's disease. *Mol Psychiatry*. 2021;26(9):5429-5440.